Hindawi Publishing Corporation
Journal of Astrophysics
Volume 2013, Article ID 838534, 7 pages
http://dx.doi.org/10.1155/2013/838534

Hindawi

Research Article

Ion-Acoustic Instabilities in a Multi-Ion Plasma

Noble P. Abraham,[1] Sijo Sebastian,[1] G. Sreekala,[1] R. Jayapal,[1] C. P. Anilkumar,[2] and Venugopal Chandu[1]

[1] *School of Pure & Applied Physics, Mahatma Gandhi University, Priyadarshini Hills, Kottayam, Kerala 686 560, India*
[2] *Equatorial Geophysical Research Laboratory, Indian Institute of Geomagnetism, Krishnapuram, Tirunelveli, Tamil Nadu 627 011, India*

Correspondence should be addressed to Venugopal Chandu; cvgmgphys@yahoo.co.in

Received 1 April 2013; Accepted 23 June 2013

Academic Editors: M. S. Dimitrijevic, A. Meli, and S. Naik

We have, in this paper, studied the stability of the ion-acoustic wave in a plasma composed of hydrogen, positively and negatively charged oxygen ions, and electrons, which approximates very well the plasma environment around a comet. Modelling each cometary component (H^+, O^+, and O^-) by a ring distribution, we find that ion-acoustic waves can be generated at frequencies comparable to the hydrogen ion plasma frequency. The dispersion relation has been solved both analytically and numerically. We find that the ratio of the ring speed ($u_{\perp s}$) to the thermal spread (v_{ts}) modifies the dispersion characteristics of the ion-acoustic wave. The contrasting behaviour of the phase velocity of the ion-acoustic wave in the presence of O^- ions for $u_{\perp s} > v_{ts}$ (and vice versa) can be used to detect the presence of negatively charged oxygen ions and also their thermalization.

1. Introduction

Low-frequency electrostatic or longitudinal ion density waves are one of the most fundamental of oscillations in a plasma [1, 2]. In the long-wavelength limit, the ions provide the inertia with the electrons as the source of the restoring force [1]. Ion-acoustic waves also exhibit strong nonlinear properties and are highly Landau damped unless $T_i \ll T_e$, where T_i and T_e are, respectively, the ion and electron temperatures [3–5]. These waves have been observed in both space and laboratory plasmas; they have thus been extensively studied in many types of high-temperature laboratory plasmas [4, 6]. The waves have been invoked to explain wave characteristics observed in Earth's ionosphere [7] and transport in the solar wind, corona, chromosphere [8], and comets [9].

In general a cometary environment contains new born hydrogen and heavier ions, with relative densities depending on the distance from the nucleus. Previous studies have concentrated on positively charged oxygen as the heavier ion species [10]. However, Giotto's observations of the inner coma of comet Halley showed that a new component, namely, negatively charged cometary ions was present, in addition to the usual thermal electrons and ions, fast cometary pickup ions, and so forth, [11]. These negative ions were observed in three broad mass peaks at 7–19, 22–65, and 85–110 amu with O^- being identified unambiguously [11].

A popular model of a cometary environment is the solar wind plasma environment permeated by dilute, drifting ring distribution of electrons and ions with finite thermal spreads [10]. Instabilities driven by an electron velocity ring distributions have been studied by many authors [12–14]. However, ion ring distributions are more important because of the greater amount of free energy available [15].

Instabilities driven by ion ring distributions have also been studied by a number of authors: close to the ion cyclotron frequency, electrostatic ion cyclotron waves propagating either perpendicularly or nearly perpendicularly to the magnetic field can be excited [16, 17]. At still higher frequencies, the magnetic effects on the ions can be neglected and lower-hybrid instabilities driven by the ring ions can occur [17–21]. And at even higher frequencies, the electrons too become unmagnetized and ion-acoustic-like instabilities result.

The frequency of the ion-acoustic wave is comparable with the ion plasma frequency and propagates parallel to the magnetic field. Generally, a combination of warm electrons

and cold ions ($T_e > T_i$) with the electrons drifting relative to the ions is the condition required to excite the ion-acoustic instability.

The ion-acoustic wave is one of the more easily observed waves in the plasma environments of comets. For example, ion-acoustic waves in the frequency range of 1.0–1.5 kHz were observed by the ICE spacecraft sent to observe the comet Giacobini-Zinner [9, Figure 3]. Again ion sound waves, with a frequency slightly less than 1 kHz, were detected by the spacecraft Sakigake which observed comet Halley [22, Figure 6].

We have, therefore, studied the stability of the ion-acoustic wave in a five-component plasma: solar wind protons, electrons, cometary hydrogen, and positively and negatively charged oxygen ions. We find that the ratio of the ring speed ($u_{\perp s}$) to the thermal spread (v_{ts}) affects the dispersion characteristics of the ion-acoustic wave. The phase velocity of the ion-acoustic wave depends sensitively on this ratio in the presence of O^- ions. This variation for $u_{\perp s} < v_{\mathrm{ts}}$ (and vice versa) is proposed as a tool for detecting the presence of O^- ions and also their thermalization.

2. The Dispersion Relation

As stated above, we intend to study the stability of the ion-acoustic wave in a five-component plasma. The five components are solar wind hydrogen and electrons and the ions of cometary origin picked up by the solar wind. These cometary ions are hydrogen and positively and negatively charged oxygen ions. The solar wind components are modelled by the Maxwellian distributions while the cometary ions are described by ring distributions.

The contributions to the dispersion relation of the plasma components described by the Maxwellian distributions are well known [23]; the same when they are described by ring distributions are given in [15]. The plasma under consideration contains components modelled by both these forms. Hence, combining these contributions, we can write down the dispersion relation for waves of frequency ω and wave vector $\vec{k}$, as

$$D\left(\omega,\vec{k}\right) = 1 + \frac{2\omega_{p\mathrm{H}^+}^2}{k^2 W_{T\mathrm{H}^+}^2}\left[1 + \xi_{\mathrm{H}^+} Z\left(\xi_{\mathrm{H}^+}\right)\right] + \frac{2\omega_{pe}^2}{k^2 W_{Te}^2}\left[1 + \xi_e Z\left(\xi_e\right)\right] - \sum_{s=\mathrm{H}^+,\,\mathrm{O}^+,\,\mathrm{O}^-} \frac{\left(\omega_{ps}^r\right)^2 \omega}{\left[\omega^2 - k_\perp^2\left(u_{\perp s} - i v_{\mathrm{ts}}\right)^2\right]^{3/2}} = 0. \quad (1)$$

In (1), $\omega_{pj} = \left[4\pi n_j e_j^2/m_j\right]^{1/2}$ and $W_{Tj} = \left[T_j/m_j\right]^{1/2}$ denote, respectively, the plasma frequency and the thermal velocity for particles of species j. Also n_j, e_j, m_j, and T_j denote, respectively, the density, charge, mass, and temperature of species j. ω_{ps}^r ($s = \mathrm{H}^+, \mathrm{O}^+, \mathrm{O}^-$) denotes the plasma frequency for the ring ions of species s while $u_{\perp s}$ and v_{ts} are, respectively, the ring ion speed and thermal spread for these ions. The plasma dispersion function $Z(\xi)$, arising from the $dv_\parallel$ integration [24], has arguments of $\xi_{\mathrm{H}^+} = \omega/kW_{T\mathrm{H}^+}$ (for hydrogen ions of solar wind origin) and $\xi_e = (\omega - kv_{ez})/kW_{Te}$ (for electrons). v_{ez} is the drift velocity of the electrons parallel to the magnetic field.

The charge neutrality condition for the plasma under consideration yields

$$\frac{n_{\mathrm{H}^+}}{n_e} = \left(1 - \frac{n_{\mathrm{H}^+}^r}{n_e} - \frac{n_{\mathrm{O}^+}^r}{n_e} + \frac{n_{\mathrm{O}^-}^r}{n_e}\right) = \left(1 - \alpha - \beta + \gamma\right), \quad (2)$$

with $\alpha = n_{\mathrm{H}^+}^r/n_e$, $\beta = n_{\mathrm{O}^+}^r/n_e$, and $\gamma = n_{\mathrm{O}^-}^r/n_e$, where n, in general, denotes the density of each species.

We derive expressions for the growth rate of the ion-acoustic wave under two limiting conditions, namely, that of a large thermal spreads ($(u_{\perp s}/v_{\mathrm{ts}}) < 1$) and small thermal spreads ($(u_{\perp s}/v_{\mathrm{ts}}) > 1$). The contributions of the solar wind hydrogen ions and electrons are the same for both cases; the contributions of the ring ions vary depending on their thermal spreads.

We use the asymptotic expansion of the plasma dispersion function $Z(\xi_{\mathrm{H}^+})$ for the solar wind hydrogen ions and the power series expansion of $Z(\xi_e)$ for the solar wind electrons. Substituting the appropriate expansions in (1), we finally arrive at the dispersion relation for ion-acoustic waves in an electron-ion plasma with three species of ring ions, as

$$\begin{aligned} D\left(\omega,\vec{k}\right) = {} & \left(1 + k^2\lambda_{De}^2\right) \\ & - \frac{\omega_{p\mathrm{H}^+}^2}{\omega^2} + i\sqrt{\pi}\frac{1}{k^2\lambda_{De}^2}\frac{1}{kW_{Te}} \\ & \times \left\{\frac{n_{\mathrm{H}^+}}{n_e}\left(\frac{m_{\mathrm{H}^+}}{m_e}\right)^{1/2}\left(\frac{T_e}{T_{\mathrm{H}^+}}\right)^{3/2}\omega e^{-\xi_{\mathrm{H}^+}^2} \right. \\ & \left. + \left(\omega - kv_{ez}\right)e^{-\xi_e^2}\right\} \\ & - \sum_{s=\mathrm{H}^+,\,\mathrm{O}^+,\,\mathrm{O}^-}\frac{n_s^r}{n_{\mathrm{H}^+}}\frac{m_{\mathrm{H}^+}}{m_s} \\ & \times \frac{\left(\omega_{p\mathrm{H}^+}\right)^2\omega}{\left[\omega^2 - k_\perp^2\left(u_{\perp s} - iv_{\mathrm{ts}}\right)^2\right]^{3/2}} = 0. \end{aligned} \quad (3)$$

In (3), $\omega = \omega_r + i\gamma$ and $\lambda_{De} = \left[T_e/(4\pi n_e e^2)\right]^{1/2}$ is the Debye length.

2.1. Case (i): Large Thermal Spreads. In this subsection we derive expressions for the real frequency and growth/damping rate for ion-acoustic waves when the thermal spreads of the ring ions are large. As a simplifying assumption we also let $\omega_r \approx k_\perp u_{\perp s}$. With the assumption of large thermal spreads

$u_{\perp s} < v_{\text{ts}}$, (3) can be simplified to yield an expression for the real frequency ω_r as

$$\omega_r^2 = \frac{(1-\alpha-\beta+\gamma)\,k^2C_s^2}{(1+k^2\lambda_{De}^2)} \times \left(1+\sum_s \alpha_s \left(\frac{u_\perp}{v_t}\right)^3 \frac{\cos((3/2)\,\theta)}{\left[1+4\left(u_\perp/v_t\right)^2\right]^{3/4}}\right) \tag{4}$$

and the growth/damping rate as

$$\gamma = -\sqrt{\frac{\pi}{8}}\frac{\omega_r^4}{\omega_{p\text{H}^+}^2 k^2\lambda_{De}^2}\frac{1}{kC_s}\frac{1}{A} \times \left[\left(\frac{n_{\text{H}^+}}{n_e}\right)\left(\frac{T_e}{T_{\text{H}^+}}\right)^{3/2} e^{-(\omega_r/kW_{T\text{H}^+})^2} - \left(\frac{m_e}{m_{\text{H}^+}}\right)^{1/2}\left(\frac{kv_{ez}}{\omega_r}-1\right)e^{-((\omega_r-kv_{ez})/kW_{Te})^2}\right] - \sum_s\left(\frac{\alpha_s}{2}\right)\omega_r\frac{(u_\perp/v_t)^3\sin((3/2)\,\theta)}{A\left[1+4\left(u_\perp/v_t\right)^2\right]^{3/4}}, \tag{5}$$

where $A = [1-\sum_s(\alpha_s/2)(u_\perp/v_t)^3(\cos((3/2)\theta)/[1+4(u_\perp/v_t)^2]^{3/4})]$.

In the above, C_s is the speed of sound defined by $C_s = [T_e/m_{\text{H}^+}]^{1/2}$, while

$$\alpha_{\text{H}^+} = \frac{n_{\text{H}^+}^r}{n_{\text{H}^+}}, \qquad \alpha_{\text{O}^+} = \frac{m_{\text{H}^+}}{m_{\text{O}^+}}\frac{n_{\text{O}^+}^r}{n_{\text{H}^+}}, \qquad \alpha_{\text{O}^-} = \frac{m_{\text{H}^+}}{m_{\text{O}^-}}\frac{n_{\text{O}^-}^r}{n_{\text{H}^+}}, \qquad \theta = \tan^{-1}\left(\frac{2u_{\perp s}}{v_{\text{ts}}}\right). \tag{6}$$

2.2. Case (ii): Small Thermal Spreads. We next consider expressions for the real frequency and the growth/damping rate when the thermal spread is small; that is, $u_{\perp s} > v_{\text{ts}}$. These can be extracted from (3) with the additional assumption $\omega_r \approx k_\perp u_{\perp s}$; the final expressions are

$$\omega_r^2 = \frac{(1-\alpha-\beta+\gamma)\,k^2C_s^2}{(1+k^2\lambda_{De}^2)}\left(1-\sum_s\left(\frac{\alpha_s}{4}\right)\left(\frac{u_\perp}{v_t}\right)^{3/2}\right), \tag{7}$$

$$\gamma = -\sqrt{\frac{\pi}{8}}\frac{\omega_r^2}{kC_s}\frac{1}{(1+k^2\lambda_{De}^2)} \times \frac{\left(1-\sum_s(\alpha_s/4)\left(u_\perp/v_t\right)^{3/2}\right)}{\left(1-\sum_s(\alpha_s/16)\left(u_\perp/v_t\right)^{3/2}\right)} \times \left[\left(\frac{n_{\text{H}^+}}{n_e}\right)\left(\frac{T_e}{T_{\text{H}^+}}\right)^{3/2} e^{-(\omega_r/kW_{T\text{H}^+})^2} - \left(\frac{m_e}{m_{\text{H}^+}}\right)^{1/2}\left(\frac{kv_{ez}}{\omega_r}-1\right)e^{-((\omega_r-kv_{ez})/kW_{Te})^2}\right] - \frac{\sum_s(\alpha_s/8)\,\omega_r\left(u_\perp/v_t\right)^{3/2}}{\left(1-\sum_s(\alpha_s/16)\left(u_\perp/v_t\right)^{3/2}\right)}. \tag{8}$$

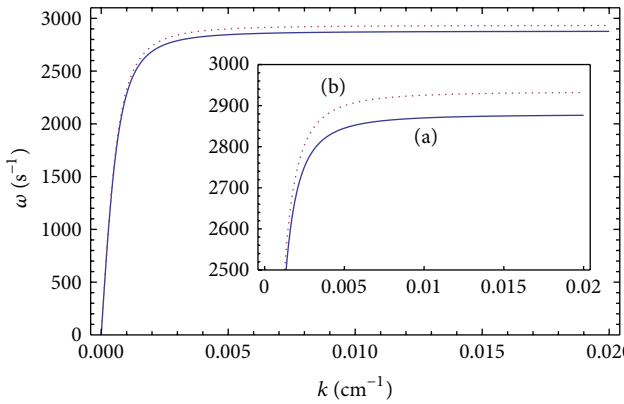

FIGURE 1: Plot of frequency ω versus wave vector $\vec{k}$. Curve (a) is for $u_{\perp s} > v_{\text{ts}}$; drift speed $u_{\perp s} = 420 \times 10^5$ cm s^{-1} and thermal spread $v_{\text{ts}} = 350\times10^5$ cm s^{-1}; curve (b) is for $u_{\perp s} < v_{\text{ts}}$; $u_{\perp s} = 100\times10^5$ cm s^{-1} and $v_{\text{ts}} = 320 \times 10^5$ cm s^{-1}.

Thus (4) and (7) are expressions for the frequencies of the ion-acoustic wave under the two limiting cases; (5) and (8) are the corresponding expressions for the growth/damping rate.

3. Results and Discussion

As a check on our results, we note from (4) and (7) the expressions for real frequency that they reduce to the corresponding ones in an electron-ion plasma when the ring ions are absent [25]. Similarly, the expressions for the growth/damping rate (5) and (8) also reduce to that in an electron-ion plasma when the ring ions are absent [25]. However what is interesting from (4) and (7) is that the real frequency is either greater (for $u_{\perp s} < v_{\text{ts}}$) or smaller (for $u_{\perp s} > v_{\text{ts}}$) than in a single ion plasma (in the absence of ring ions). The electron drift velocity, parallel to the magnetic field, is the source of energy for the instability. Thus, for a given wave vector $\vec{k}$ and ion densities, a greater drift velocity of the electrons is required to drive the wave unstable in the case where the thermal spread of the ring ions is large.

We use parameters similar to that in [10]. The solar wind hydrogen density $n_{\text{H}^+} = 4.95\,\text{cm}^{-3}$, while the hydrogen and electron temperatures are $T_{\text{H}^+} = 8\times10^{4^\circ}\text{K}$, $T_e = 2\times10^{5^\circ}\text{K}$. The densities of the ring ions are $n_{\text{H}^+}^r = 0.5\,\text{cm}^{-3}$, $n_{\text{O}^+}^r = 0.25\,\text{cm}^{-3}$, and $n_{\text{O}^-}^r = 0.05\,\text{cm}^{-3}$.

Ion-acoustic waves were observed in the frequency range from 1.0 to 1.5 kHz by the ICE spacecraft at the comet Giocobini-Zinner [9]. Thus to calculate the wave vector $\vec{k}$, a frequency of $\omega = 1.4$ kHz was used in the cold plasma dispersion relation and the wave vector $\vec{k}$ was calculated. $\vec{k}$ was then varied around this value in subsequent calculations.

Figure 1 is a plot of the frequency ω versus wave vector $\vec{k}$, with the frequency ω being obtained by solving (4) and (7). Curve (a) has a drift speed $u_{\perp s} = 420 \times 10^5$ cm s^{-1} and a thermal spread of $v_{\text{ts}} = 350 \times 10^5$ cm s^{-1} ($u_{\perp s} > v_{\text{ts}}$) while for curve (b) $u_{\perp s} = 100\times10^5$ cm s^{-1}, $v_{\text{ts}} = 320\times10^5$ cm s^{-1} ($u_{\perp s} < v_{\text{ts}}$). As is evident from the figure the waves are at a higher

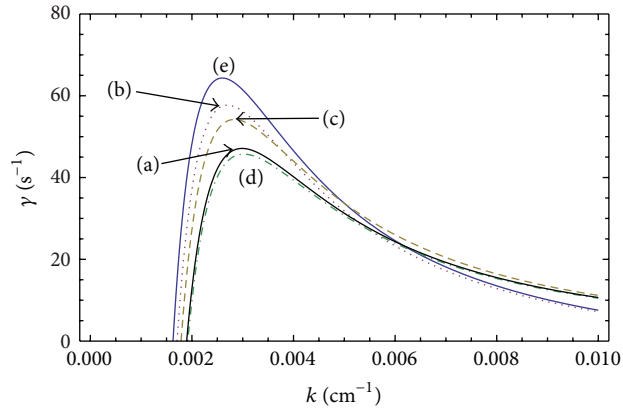

FIGURE 2: Plot of the growth rate γ (5) versus wave vector $\vec{k}$ for $T_e = 2 \times 10^5$°K, $T_{H^+} = 8 \times 10^4$°K, $u_{\perp s} = 100 \times 10^5$ cm s^{-1}, $v_{ts} = 320 \times 10^5$ cm s^{-1}, and an electron drift speed $v_{ez} = 2460 \times 10^5$ cm s^{-1}. Curve (a) is for a single ion plasma without any ring ions. Curve (b) has a H^+ ring, curve (c) has an O^+ ring, curve (d) has an O^- ring, and for curve (e) all species of ring ions are present.

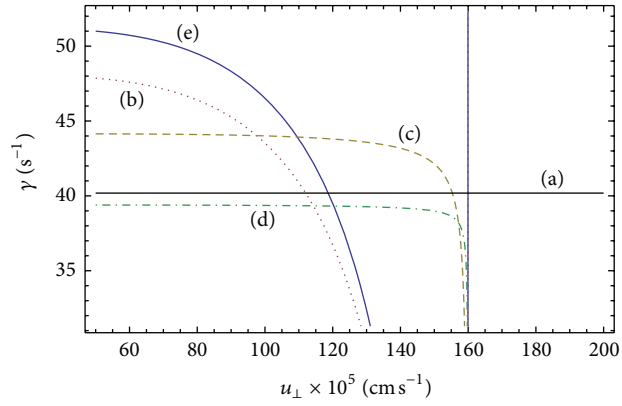

FIGURE 3: Plot of the growth rate γ (5) versus $u_{\perp s}$ ($v_{ts} = 320 \times 10^5$ cm s^{-1}, $\vec{k} = 0.004$ cm^{-1}). Other relevant parameters are the same as in Figure 2. Curve (a) is for a single ion plasma without any ring ions. Curve (b) is for a H^+ ring, curve (c) has an O^+ ring, and curve (d) is for an O^- ring. Curve (e) depicts the case when all species of ring ions are present.

frequency for $u_{\perp s} < v_{ts}$. Since the calculated frequencies are in better agreement with the observed range of frequencies for $u_{\perp s} > v_{ts}$, it is safe to assume that thermalization of the ring ions has not yet occurred. The pickup of new born ions by the solar wind has been described by a three-step process: formation of a ring beam distribution, pitch angle scattering of this initial distribution into a shell, and a slower velocity diffusion that spreads out the shell [26].

We first consider the growth/damping rates when the thermal spread is large.

Figure 2 is a plot of the growth rate γ (5) versus wave vector $\vec{k}$ for $T_e = 2 \times 10^5$°K, $T_{H^+} = 8 \times 10^4$°K, $u_{\perp s} = 100 \times 10^5$ cm s^{-1}, $v_{ts} = 320 \times 10^5$ cm s^{-1}, and an electron drift speed $v_{ez} = 2460 \times 10^5$ cm s^{-1}. Curve (a) is for a single ion plasma without ring distributions. Curve (b) has only one type of ring

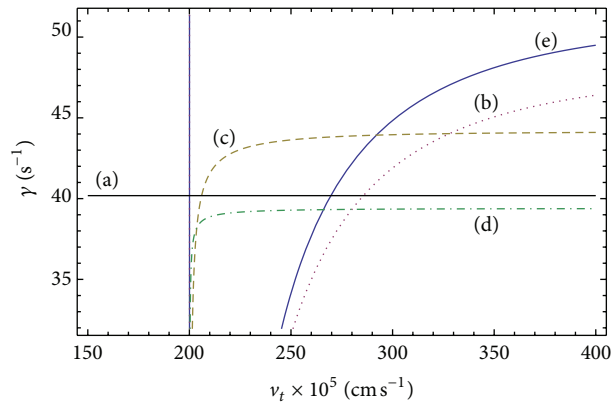

FIGURE 4: Plot of the growth rate γ (5) versus v_{ts} ($u_{\perp s} = 100 \times 10^5$ cm s^{-1}, $\vec{k} = 0.004$ cm^{-1}). Other relevant parameters are the same as in Figure 2. Curve (a) is for a single ion plasma without any ring ions. Curve (b) has a H^+ ring, curve (c) has an O^+ ring, curve (d) has an O^- ring, and for curve (e) all species of ring ions are present.

distribution, namely, the H^+ ring. We find that the growth rate is enhanced. Curve (c) is for the O^+ ring replacing the H^+ ring—there is a slight decrease in the growth rate. When this single ring is the O^- ring, the growth rate is the lowest (curve (d)). The growth rate is also shown when all species of rings are present (curve (e)). The ion-acoustic wave is thus driven unstable by the electrons drifting parallel to the magnetic field (addition of negative ions reduces the density of electrons required to maintain charge neutrality); the ring ions add to the instability, with the lighter ion hydrogen ring being the most effective in enhancing the instability of the wave.

Figures 3 and 4 depict the variation of the growth rate γ (5) versus $u_{\perp s}$ ($v_{ts} = 320 \times 10^5$ cm s^{-1}) (Figure 3) or γ versus v_{ts} ($u_{\perp s} = 100 \times 10^5$ cm s^{-1}) (Figure 4), with the temperatures and electron drift speed being the same as in Figure 2. In both figures curve (a) represents the growth rate in a single ion plasma (ring ions are not present); curve (b) when the H^+ ring alone is present, curve (c) when the O^+ ring alone is present, and curve (d) when an O^- ring alone is present. Curve (e) is for the situation when all species of ring ions are present. While the general nature of the curves is similar to that in Figure 2, the heavier ion rings extend the range of $u_{\perp s}$ and v_{ts} over which the wave is unstable as compared to the lighter ion ring alone being present.

We next consider the case of low thermal spreads ($u_{\perp s} > v_{ts}$).

Figure 5 is a plot of the growth rate (8) versus wave vector $\vec{k}$ for $T_e = 2 \times 10^5$°K, $T_{H^+} = 8 \times 10^4$°K, $u_{\perp s} = 420 \times 10^5$ cm s^{-1}, $v_{ts} = 350 \times 10^5$ cm s^{-1}, and an electron drift speed $v_{ez} = 2460 \times 10^5$ cm s^{-1}. Similar to Figure 2, curve (a) is for a single ion plasma without any ring ions. Curve (b) is for the H^+ ring and has the lowest growth rate. Curve (c) is for the O^+ ring replacing the H^+ ring—there is an enhancement in the growth rate, than the single ion plasma. When this single ring is the O^- ring, the growth rate is slightly lowered (curve (d)). Curve (e) shows the growth rate when all the species of rings are present. The ion-acoustic wave is thus

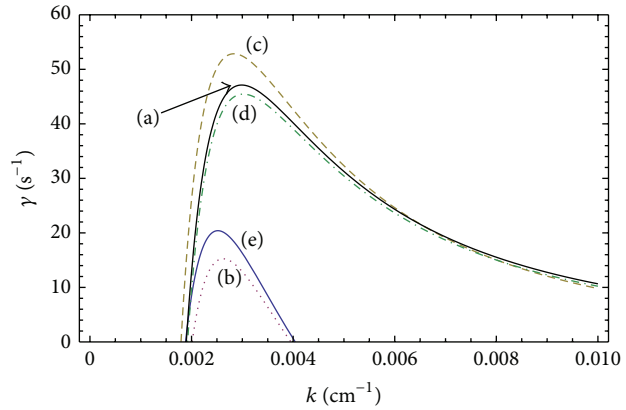

FIGURE 5: Plot of the growth rate γ (8) versus wave vector $\vec{k}$ for $T_e = 2 \times 10^{5}$°K, $T_{H^+} = 8 \times 10^{4}$°K, $u_{\perp s} = 420 \times 10^5$ cm s^{-1}, $v_{ts} = 350 \times 10^5$ cm s^{-1}, and an electron drift speed $v_{ez} = 2460 \times 10^5$ cm s^{-1}. Curve (a) is for a single ion plasma without any ring ions. Curve (b) has a H^+ ring, curve (c) has an O^+ ring, and curve (d) has an O^- ring. Curve (e) has all species of ring ions.

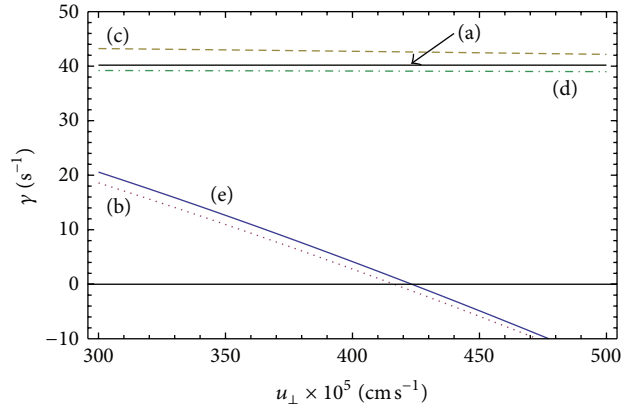

FIGURE 6: Plot of the growth rate γ (8) versus $u_{\perp s}$ ($v_{ts} = 350 \times 10^5$ cm s^{-1}, $\vec{k} = 0.004$ cm^{-1}). Other parameters are the same as in Figure 5. Curve (a) is for a single ion plasma without any ring ions. Curve (b) has a H^+ ring, curve (c) has an O^+ ring, curve (d) has an O^- ring, and curve (e) has all species of ring ions.

again driven unstable by the electrons drifting parallel to the magnetic field (addition of negative ions reduces the density of electrons required to maintain charge neutrality); the ring ions generally reduce the growth with the lighter ion hydrogen ring being the most effective in damping the wave.

Figures 6 and 7 depict the variation of the growth rate γ (8) versus $u_{\perp s}$ ($v_{ts} = 350 \times 10^5$ cm s^{-1}) (Figure 6) or γ versus v_{ts} ($u_{\perp s} = 420 \times 10^5$ cm s^{-1}) (Figure 7), with the temperatures and drift speed being the same as in Figure 5. In both figures, labelling of the curves is similar to that in Figures 3 and 4. While the general nature of the curves is similar to that in Figure 5, the heavier ion rings have much larger ranges of $u_{\perp s}$ and v_{ts} over which the wave is unstable.

In a recent study Misra et al. [27] investigated the propagation characteristics of the dust ion-acoustic (DIA) waves in a collisional, negative ion plasma with immobile,

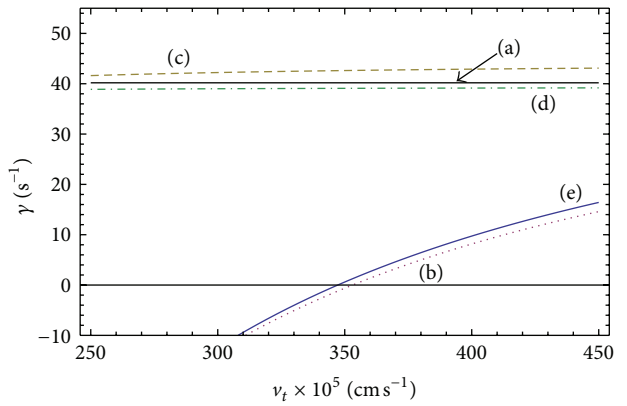

FIGURE 7: Plot of the growth rate γ (8) versus v_{ts} ($u_{\perp s} = 420 \times 10^5$ cm s^{-1}, $\vec{k} = 0.004$ cm^{-1}). Other relevant parameters are the same as in Figure 5. Curve (a) is for a single ion plasma without any ring distributions. Curve (b) has a H^+ ring, curve (c) has an O^+ ring, curve (d) has an O^- ring, and curve (e) has all species of ring ions.

charged dust grains. In the linear regime, they found two modes—the "fast" and "slow" modes. They also found that the Landau damping effect on the fast mode was negligible while the slow mode was stable.

Our dispersion diagram (Figure 1) also reveals the existence of two modes—a "slow" mode (curve (a) of Figure 1 with $u_{\perp s} > v_{ts}$) and a "fast" mode (curve (b), Figure 1 with $u_{\perp s} < v_{ts}$). Also as mentioned in Section 1, ion-acoustic waves were observed in the frequency range of 1.0–1.5 kHz at comet Giacobini-Zinner [9] and at a frequency slightly lesser than 1.0 kHz at comet Halley [22]. The waves are also expected to saturate at frequencies below the local ion plasma frequency [28]. A comparison of the growth rate for the fast (Figures 2, 3, and 4) and the slow (Figures 5, 6, and 7) modes reveals that the growth rate of the fast mode is much larger when compared to that of the slow mode. Thus, while the slow mode in [27] was freely propagating, the slow mode in the plasma under consideration is weakly unstable. It may be noted here that this study uses the full kinetic treatment and hence can also be considered as a generalisation of the fluid treatment in [27].

Finally Figure 8 depicts the variation of the real frequency versus the wave vector $\vec{k}$. The panel at the top is for the fast wave ($u_{\perp s} < v_{ts}$, $u_{\perp s} = 100 \times 10^5$ cm s^{-1}, $v_{ts} = 320 \times 10^5$ cm s^{-1}); curve (a) is for the case when there are no heavier ions ($n_{H^+} = 4.95$ cm^{-3}, $n^r_{H^+} = 0.5$ cm^{-3}) while curve (b) depicts the situation where negatively charged oxygen is also added ($n_{H^+} = 4.95$ cm^{-3}, $n^r_{H^+} = 0.5$ cm^{-3}, and $n^r_{O^-} = 0.2$ cm^{-3}). We find that the addition of O^- increases the frequency and hence the phase velocity of the ion-acoustic wave. The lower panel is for the slow wave ($u_{\perp s} > v_{ts}$, $u_{\perp s} = 420 \times 10^5$ cm s^{-1}, $v_{ts} = 350 \times 10^5$ cm s^{-1})—curve (c) is for the case where only the lighter ions are present ($n_{H^+} = 4.95$ cm^{-3}, $n^r_{H^+} = 0.5$ cm^{-3}) and curve (d) depicts the situation when O^- is also added ($n_{H^+} = 4.95$ cm^{-3}, $n^r_{H^+} = 0.5$ cm^{-3}, and $n^r_{O^-} = 0.2$ cm^{-3}). The decrease in the frequency and thereby the phase velocity is distinctly evident from the figure.

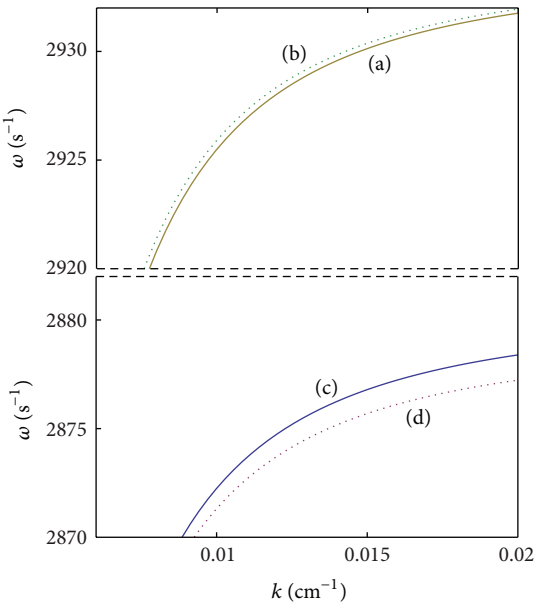

FIGURE 8: Plot of frequency ω versus wave vector $\vec{k}$. The panel at the top is for the fast wave ($u_{\perp s} < v_{ts}$; $u_{\perp s} = 100 \times 10^5$ cm s^{-1}, $v_{ts} = 320 \times 10^5$ cm s^{-1}) of Figure 1: curve (a) is for the case when there are no heavier ions ($n_{H^+} = 4.95$ cm^{-3}, $n^r_{H^+} = 0.5$ cm^{-3}) while curve (b) depicts the situation when negatively charged oxygen is also added ($n_{H^+} = 4.95$ cm^{-3}, $n^r_{H^+} = 0.5$ cm^{-3}, and $n^r_{O^-} = 0.2$ cm^{-3}). The lower panel is for the slow wave ($u_{\perp s} > v_{ts}$; $u_{\perp s} = 420 \times 10^5$ cm s^{-1}, $v_{ts} = 350 \times 10^5$ cm s^{-1}) of Figure 1: curve (c) is for the case where only the lighter ions are present ($n_{H^+} = 4.95$ cm^{-3}, $n^r_{H^+} = 0.5$ cm^{-3}) and curve (d) depicts the situation when O^- is also added ($n_{H^+} = 4.95$ cm^{-3}, $n^r_{H^+} = 0.5$ cm^{-3}, and $n^r_{O^-} = 0.2$ cm^{-3}). Other relevant parameters are the same as in Figure 1.

Variation of the phase velocity of ion-acoustic waves has been proposed as a diagnostic tool for the detection of charged dust grains in laboratory plasmas [28, 29]. We thus propose to extend this idea—the contrasting behaviour of the phase velocity of the ion-acoustic wave in the presence of O^- ions for $u_{\perp s} > v_{ts}$ (and vice versa) can be used not only to detect the presence of negatively charged oxygen ions but also their thermalization as well.

4. Conclusions

We have studied the stability of the ion-acoustic waves in a five-component plasma, which approximates very well the plasma environment around a comet. The five components are solar wind hydrogen and electrons and the ions of cometary origin. The cometary ions are hydrogen and positively and negatively charged oxygen ions. The solar wind components are modelled by the Maxwellian distributions while the cometary ions are described by ring distributions. We find that the ion-acoustic waves can be generated at frequencies comparable to the observed frequency. The ratio of the ring speed to its thermal spread modifies the dispersion characteristics of the ion-acoustic wave. When the thermal spread is large compared to the ring speed ($v_{ts} > u_{\perp s}$), the ring ions enhance the instability of the ion-acoustic wave. The growth rate is lowered when the thermal spread is smaller in comparison with the ring speed ($u_{\perp s} > v_{ts}$). We also find that heavier ring ions extend the range of $u_{\perp s}$ and v_{ts} over which the wave is unstable when compared to the lighter ring ions. The contrasting behaviour of the phase velocity of the ion-acoustic wave in the presence of O^- ions for $u_{\perp s} > v_{ts}$ (and vice versa) can be used to detect the presence of negatively charged oxygen ions and also their thermalization.

Acknowledgments

The authors thank the referees for their valuable comments. Financial assistance from the University Grants Commission (SAP) and Department of Science and Technology (FIST and PURSE Programs) is gratefully acknowledged.

References

[1] J. Castro, P. McQuillen, and T. C. Killian, "Ion acoustic waves in ultracold neutral plasmas," *Physical Review Letters*, vol. 105, no. 6, Article ID 065004, 2010.

[2] L. Tonks and I. Langmuir, "Oscillations in ionized gases," *Physical Review*, vol. 33, no. 2, pp. 195–210, 1929.

[3] T. H. Stix, *Waves in Plasmas*, American Institute of Physics, New York, NY, USA, 2nd edition, 1992.

[4] Y. Nakamura, H. Bailung, and P. K. Shukla, "Observation of ion-acoustic shocks in a dusty plasma," *Physical Review Letters*, vol. 83, no. 8, pp. 1602–1605, 1999.

[5] Z. Liu, L. Liu, and J. Du, "A nonextensive approach for the instability of current-driven ion-acoustic waves in space plasmas," *Physics of Plasmas*, vol. 16, no. 7, Article ID 072111, 5 pages, 2009.

[6] M. Yamada and M. Raether, "Saturation of the ion-acoustic instability in a weakly ionized plasma," *Physical Review Letters*, vol. 32, no. 3, pp. 99–102, 1974.

[7] M. E. Koepke, "Contributions of Q-machine experiments to understanding auroral particle acceleration processes," *Physics of Plasmas*, vol. 9, no. 5, pp. 2420–2427, 2002.

[8] S. R. Cranmer, A. A. Van Ballegooijen, and R. J. Edgar, "Self-consistent coronal heating and solar wind acceleration from anisotropic magnetohydrodynamic turbulence," *Astrophysical Journal, Supplement Series*, vol. 171, no. 2, pp. 520–551, 2007.

[9] F. L. Scarf, F. V. Coroniti, C. F. Kennel, D. A. Gurnett, W.-H. Ip, and E. J. Smith, "Plasma wave observations at comet Giacobini-Zinner," *Science*, vol. 232, no. 4748, pp. 377–381, 1986.

[10] A. L. Brinca and B. T. Tsurutani, "Unusual characteristics of electromagnetic waves excited by cometary newborn ions with large perpendicular energies," *Astronomy & Astrophysics* , vol. 187, no. 1-2, pp. 311–319, 1987.

[11] P. Chaizy, H. Rème, J. A. Sauvaud et al., "Negative ions in the coma of comet Halley," *Nature*, vol. 349, no. 6308, pp. 393–396, 1991.

[12] T. J. Tataronis and F. Crawford, "Cyclotron harmonic wave propagation and instabilities," *Journal of Plasma Physics*, vol. 4, no. 2, pp. 231–264, 1970.

[13] M. Ashour-Abdalla and C. F. Kennel, "Nonconvective and convective electron cyclotron harmonic instabilities," *Journal of Geophysical Research*, vol. 83, p. 1531, 1978.

[14] P. Sprangle, J. L. Vomvoridis, and W. M. Manheimer, "A classical electron cyclotron quasioptical maser," *Applied Physics Letters*, vol. 38, no. 5, pp. 310–313, 1981.

[15] K. Akimoto, K. Papadopoulos, and D. Winske, "Ion-acoustic instabilities driven by an ion velocity ring," *Journal of Plasma Physics*, vol. 34, no. 3, pp. 467–479, 1985.

[16] J. A. Byers and M. Grewal, "Perpendicularly propagating plasma cyclotron instabilities simulated with a one-dimensional computer model," *Physics of Fluids*, vol. 13, no. 7, pp. 1819–1830, 1970.

[17] J. K. Lee and C. K. Birdsall, "Velocity space ring-plasma instability, magnetized, part I: theory," *Physics of Fluids*, vol. 22, no. 7, pp. 1306–1314, 1979.

[18] S. Seiler, M. Yamada, and H. Ikezi, "Lower hybrid instability driven by a spiraling ion beam," *Physical Review Letters*, vol. 37, no. 11, pp. 700–703, 1976.

[19] H. E. Mynick, M. J. Gerver, and C. K. Birdsall, "Stability regions and growth rates for a two-ion component plasma, unmagnetized," *Physics of Fluids*, vol. 20, no. 4, pp. 606–612, 1977.

[20] C. Cattel and M. Hudson, "Flute mode waves near ω_{LH} excited by ion rings in velocity space," *Geophysical Research Letters*, vol. 9, no. 10, pp. 1167–1170, 1982.

[21] K. Akimoto, K. Papadopoulos, and D. Winske, "Lower-hybrid instabilities driven by an ion velocity ring," *Journal of Plasma Physics*, vol. 34, no. 3, pp. 445–465, 1985.

[22] F. Scarf, "Plasma wave observations at comets Giacobini-Zinner and Halley," in *Plasma Waves and Instabilities at Comets and in Magnetospheres*, B. T. Tsurutani and H. Oya, Eds., American Geophysical Union, Washington, DC, USA, 1989.

[23] R. C. Davidson, "Kinetic waves and instabilities in a uniform plasma," in *Basic Plasma Physics*, A. Galeev and R. Sudan, Eds., North-Holland, New York, NY, USA, 1989.

[24] B. D. Fried and S. D. Conte, *The Plasma Dispersion Function*, Academic Press, New York, NY, USA, 1961.

[25] D. A. Gurnnet and A. Bhattacharjee, *Introduction to Plasma Physics: with Space and Laboratory Applications*, Cambridge University Press, Cambridge, UK, 1st edition, 2005.

[26] J. D. Gaffey Jr, D. Winske, and C. S. Wu, "Time scales for formation and spreading of velocity shells of pickup ions in the solar wind," *Journal of Geophysical Research*, vol. 93, no. A6, pp. 5470–5486, 1988.

[27] A. P. Misra, N. C. Adhikary, and P. K. Shukla, "Ion-acoustic solitary waves and shocks in a collisional dusty negative-ion plasma," *Physical Review E*, vol. 86, no. 5, Article ID 056406, 10 pages, 2012.

[28] S. H. Kim and R. L. Merlino, "Charging of dust grains in a plasma with negative ions," *Physics of Plasmas*, vol. 13, no. 5, Article ID 052118, 7 pages, 2006.

[29] M. Rosenberg and R. L. Merlino, "Ion-acoustic instability in a dusty negative ion plasma," *Planetary and Space Science*, vol. 55, no. 10, pp. 1464–1469, 2007.